DOE/ER/13846--4

DE93 001836

II. PROGRESS REPORT #4

The research described in this proposal will be the continuation of the ongoing research which is currently being supported by the U.S. Department of Energy under the contract "Mathematical Models of Hysteresis" (contract No. DE-FG05-88ER13846). Thus, before discussing the proposed research in detail, it is worthwhile to describe and summarize the main results achieved in the course of our work under the above contract.

Our ongoing research has largely been focused on the development of mathematical models of hysteretic nonlinearities with "nonlocal memories". The distinct feature of these nonlinearities is that their current states depend on past histories of input variations. It turns out that memories of hysteretic nonlinearities are quite selective. Indeed, experiments show that only some past input extrema (not the entire input variations) leave their marks upon future states of hysteretic nonlinearities. Thus special mathematical tools are needed in order to describe nonlocal selective memories of hysteretic nonlinearities. The origin of such tools can be traced back to the landmark paper of Preisach.

Our research has been primarily concerned with Preisach-type models of hysteresis. All these models have a common generic feature; they are constructed as superpositions of simplest hysteretic nonlinearities-rectangular loops. Our study has by and large been centered around the following topics: various generalizations and extensions of the classical Preisach model (with special emphasis on vector generalizations), finding of necessary and sufficient conditions for the representation of actual hysteretic nonlinearities by various Preisach type models, solution of identification problems for these models, numerical implementation and experimental testing of Preisach type models. Although the study of Preisach type models has constituted the main direction of the research, some effort has also been made to establish some interesting connections between these models and such topics as: the critical state model for superconducting hysteresis, the classical Stoner-Wohlfarth model of vector magnetic hysteresis, thermal activation type models for viscosity, magnetostrictive hysteresis and neural networks.

We begin our description of the achieved results with the following definition of the classical Preisach model. Consider an infinite set of simplest hysteresis operators $\hat{\gamma}_{\alpha\beta}$. Each of these operators can be represented by a rectangular loop on the input-output diagram

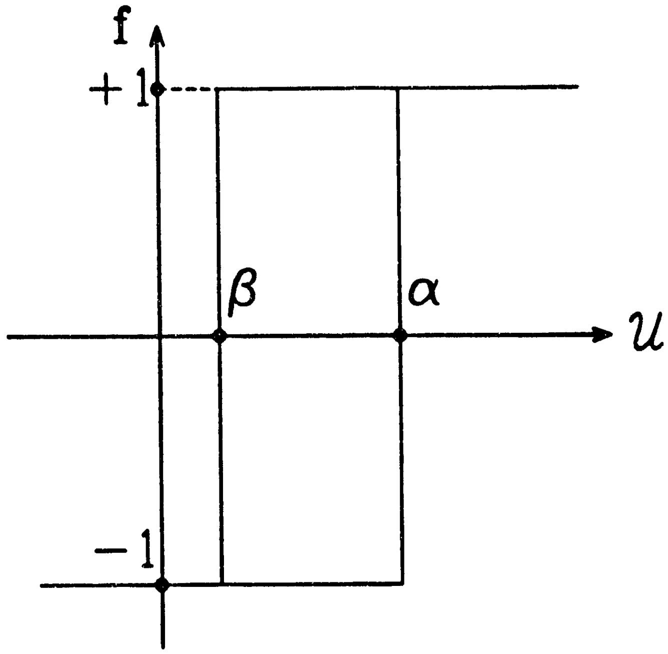

Fig. 1

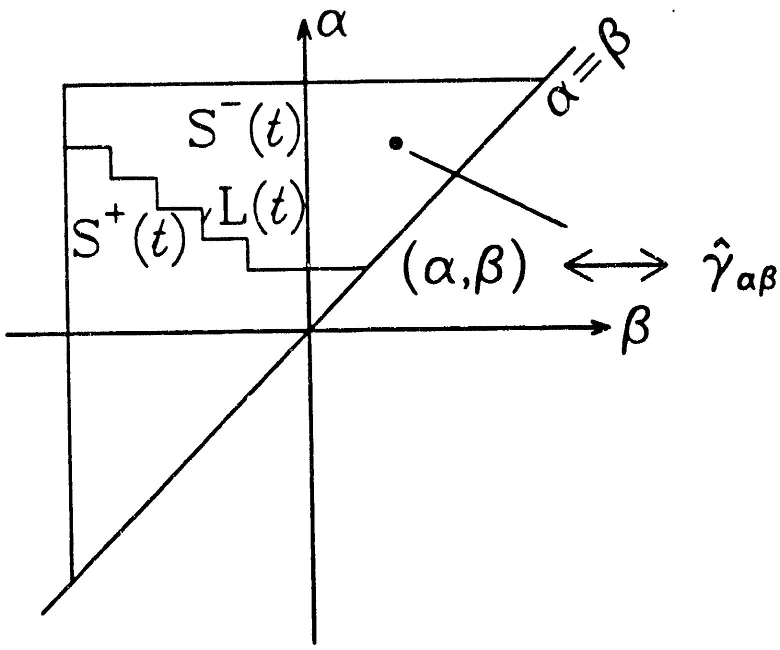

Fig. 2

(see Figure 1). Numbers α and β correspond to "up" and "down" switching values of input, respectively. Outputs of the above elementary hysteresis operators may assume only two values, $+1$ and -1. Along with the set of operators $\hat{\gamma}_{\alpha\beta}$ consider an arbitrary weight function $\mu(\alpha, \beta)$. Then, the Preisach model can be written as follows

$$f(t) = \hat{\Gamma}u(t) = \iint_{\alpha>\beta} \mu(\alpha, \beta)\hat{\gamma}_{\alpha\beta}u(t)d\alpha d\beta \tag{1}$$

In the sequel, the case when $\mu(\alpha, \beta)$ is a finite function with a support within some triangle $T : (\beta_0 \leq \beta \leq \alpha \leq \alpha_0)$ will be discussed. This case includes the important class of nonlinearities with major hysteresis loops.

The understanding of the classical Preisach model is considerably facilitated by its geometric interpretation. This interpretation is based on the simple fact that there is a one-to-one correspondence between operators $\hat{\gamma}_{\alpha\beta}$ and points (α, β) of the half plane $\alpha \geq \beta$. By using this fact, it can be shown that at any instant of time, the triangle T is subdivided into two sets (see Fig. 2): $S^+(t)$ consisting of points (α, β) for which $\hat{\gamma}_{\alpha\beta}u(t) = 1$ and $S^-(t)$ consisting of points (α, β) for which $\hat{\gamma}_{\alpha\beta}u(t) = -1$. It can also be shown that the interface $L(t)$ between $S^+(t)$ and $S^-(t)$ is a staircase line whose vertices have α and β coordinates coinciding with some local maxima and minima of input at previous instants of time. The final link of $L(t)$ is attached to the line $\alpha = \beta$ and moves when the input changes. This link is a horizontal one and moves upwards when the input increases, and it is a vertical one and moves from right to left when the input decreases. By using the above geometric interpretation, the mode (1) can be represented in the following equivalent form:

$$f(t) = \iint_{S^+(t)} \mu(\alpha, \beta)d\alpha d\beta - \iint_{S^-(t)} \mu(\alpha, \beta)d\alpha d\beta. \tag{2}$$

From expression (2), it is clear that an instantaneous value of output depends on the shape of the interface $L(t)$, which in turn is determined by the extremum values of input at previous instants of time. Consequently, the past extremum values of input shape the interface $L(t)$, and in this way, they leave their mark upon the future values of output.

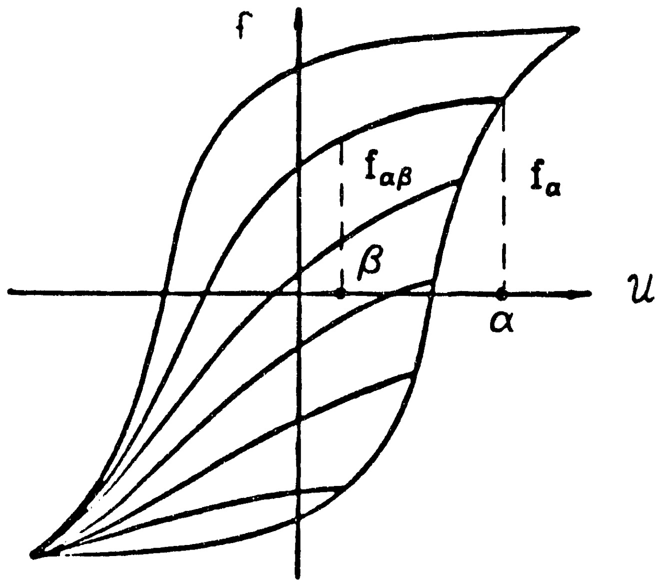

Fig. 3

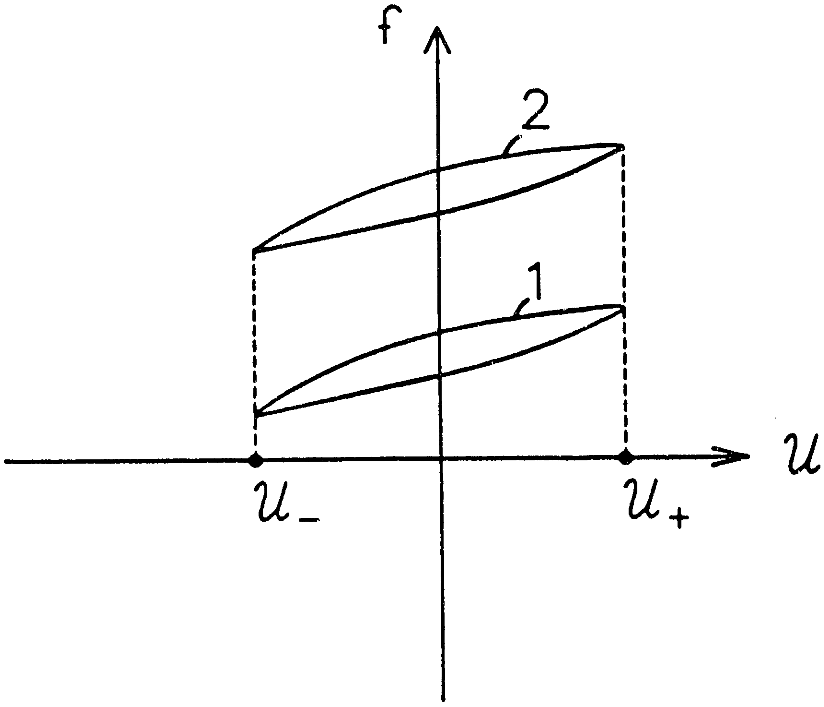

Fig. 4

To determine $\mu(\alpha, \beta)$ (this is the so-called identification problem), a set of experimentally measured first-order transition (reversal) curves should be employed. These first-order transition curves are shown in Figure 3. By using these curves, we can define the function:

$$F(\alpha, \beta) = f_{\alpha} - f_{\alpha\beta} \tag{3}$$

It can be shown that by knowing $F(\alpha, \beta)$, the function $\mu(\alpha, \beta)$ can be determined from the formula:

$$\mu(\alpha, \beta) = -\frac{1}{2}\frac{\partial^2 F(\alpha, \beta)}{\partial\alpha\partial\beta} \tag{4}$$

It turns out that not all extremum input values are accumulated by the model (1); some of them can be wiped out. More precisely, it can be shown (by using the rules of motion of the final link of $L(t)$) that the following fact is valid.

Property A(wiping-out property). Each local maximum wipes out the vertices whose α coordinates are below this maximum, and each local minimum wipes out the vertices whose β coordinates are above this minimum.

Another characteristic property of the model (1) is illustrated by Figure 4. It can be stated as follows:

Property B (congruency property). All minor hysteresis loops corresponding to the same extremum values of input are congruent.

The following result has been proven (see [1]).

Theorem. Properties A and B constitute necessary and sufficient conditions for a hysteretic nonlinearity to be represented by the model (1) on the set of piece-wise monotonic inputs.

The above theorem clearly reveals the limits of applicability of the classical Preisach model. This theorem and the given definition of the classical Preisach model show that this model has the following intrinsic limitations.

1. The classical Preisach model describes hysteretic nonlinearities which exhibit congruency of minor loops formed for the same reversal values of input. However, many experiments show that actual hysteretic nonlinearities may substantially deviate from this property.

2. The classical Preisach model is static in nature and does not account for dynamic properties of hysteretic nonlinearities. However, for fast input variations these properties may be essential.

3. The classical Preisach model describes hysteretic nonlinearities with wiping out property. This property is tantamount to the immediate formation of hysteresis loop after only one cycle of back-and-forth variation of input between any two reversal values. However, experiments show that hysteresis loop formation is often preceded by some stabilization process which may require large number of cycles to achieve a stable minor loop. This process is also called in the literature "accommodation" or "reptation" process .

4. The classical Preisach model deals only with scalar hysteretic nonlinearities. However, in many applications vector hysteresis is encountered. Properties of this hysteresis are usually quite different from scalar hysteresis properties.

To remove (or relax) the above mentioned limitations, essential generalizations of the classical Preisach model are needed. These generalizations have been the main focus of our ongoing research. We shall first describe some interesting modification of the classical Preisach model [2]. This modification reveals that the Preisach model does describe to a certain extent reversible properties of hysteresis nonlinearities. This fact has been overlooked in the existing literature. Apart from the mentioned fact, this modification has been also instrumental in the further generalizations of the classical Preisach model which are discussed below.

Consider the subdivision of the triangle T into three sets $S^+_{u(t)}, R_{u(t)}$ and $S^-_{u(t)}$ (see Figure 5), which are defined as:

$$
\begin{aligned}
&(\alpha,\beta)\epsilon S^+_{u(t)}, \quad \text{if} \quad \beta_0 \le \beta \le \alpha \le u(t),\\
&(\alpha,\beta)\epsilon R_u(t), \quad \text{if} \quad \beta_0 \le \beta \le u(t), \quad u(t) \le \alpha \le \alpha_0,\\
&(\alpha,\beta)\epsilon S^-_{u(t)}, \quad \text{if} \quad u(t) \le \beta \le \alpha \le \alpha_0.
\end{aligned} \tag{5}
$$

By using the above subdivision and some transformations, the classical Preisach model (1)

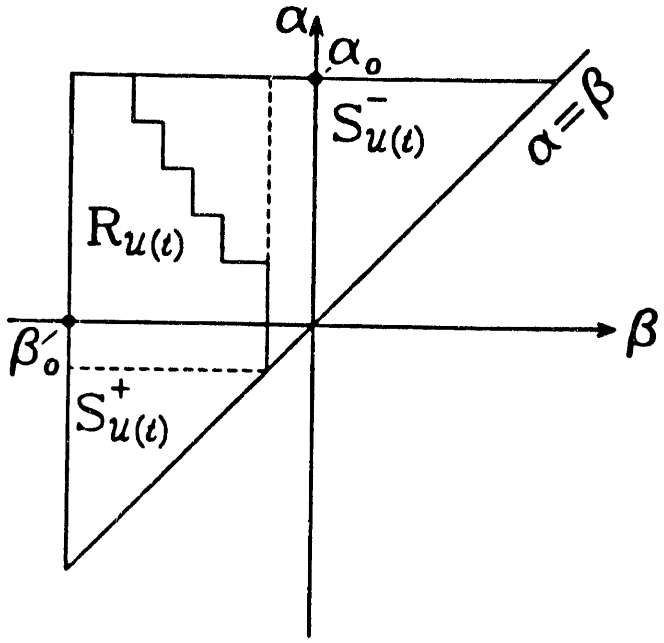

Fig. 5

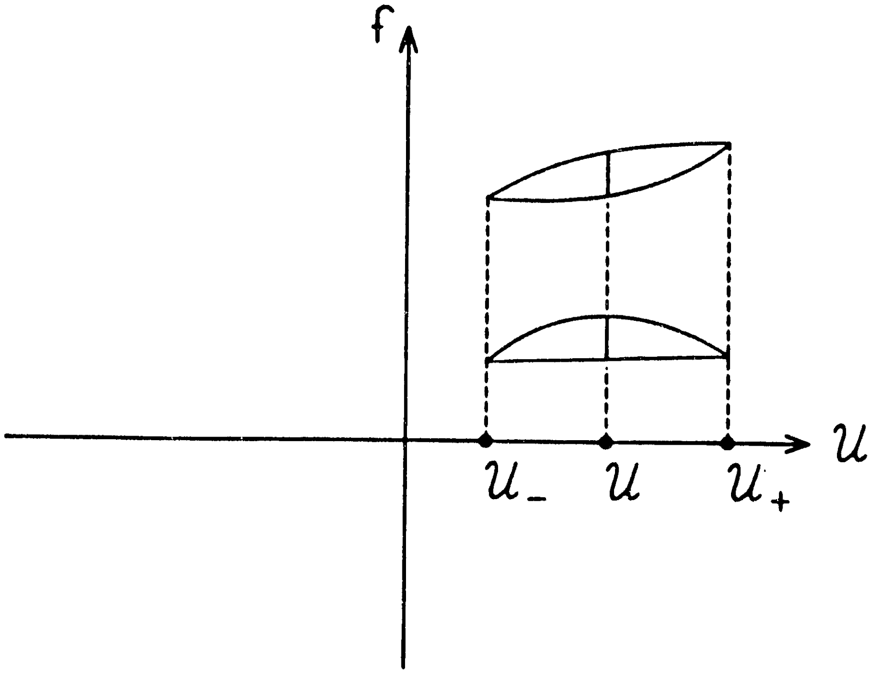

Fig. 6

can be represented as follows:

$$f(t) = \iint\limits_{R_{u(t)}} \mu(\alpha,\beta)\hat{\gamma}_{\alpha\beta}u(t)d\alpha d\beta + \frac{1}{2}(f^{+}_{u(t)} + f^{-}_{u(t)}). \tag{6}$$

The last expression is formally equivalent to the classical Preisach model (1). However, in this expression the integration is performed not over the fixed triangle T but over the rectangle $R_{u(t)}$ which changes along with input variations. For this reason, the expression (6) can be termed as a moving Preisach model. It is also clear from (6) that $\frac{1}{2}(f^{+}_{u(t)} + f^{-}_{u(t)})$ represents a fully reversible component of hysteretic nonlinearity described by the classical Preisach model. In this respect, the first term in the right-hand side of (6) can be construed as irreversible component of the classical Preisach model.

We next discuss the nonlinear (input dependent) Preisach model of hysteresis [3]. This model can be mathematically defined as:

$$f(t) = \iint\limits_{R_{u(t)}} \mu(\alpha,\beta,u(t))\hat{\gamma}_{\alpha\beta}u(t)d\alpha d\beta + \frac{f^{+}_{u(t)} + f^{-}_{u(t)}}{2}. \tag{7}$$

It is clear that a new feature of this model in comparison with the moving model (6) is the dependence of the distribution function μ on the current value of input, $u(t)$. For this reason, the model (7) is termed as the nonlinear or input dependent Preisach model. Due to the new feature mentioned above, the first term in the right-hand side of (7) can be construed as a partially reversible component of hysteretic nonlinearity. Indeed, for each pair (α,β), the integrand $\mu(\alpha,\beta,u(t))\hat{\gamma}_{\alpha\beta}u(t)$ is reversible for input variations between α and β.

The nonlinear Preisach model admits a geometric interpretation which is similar to that for the classical model. As a result, the same Wiping-Out Properties (Property A) is valid for the model (7) as for the classical Preisach model. However, the Congruency Property (Property B) is essentially relaxed for the nonlinear mode (7). Namely, the following property is valid.

Property C (Property of Equal Vertical Chords)

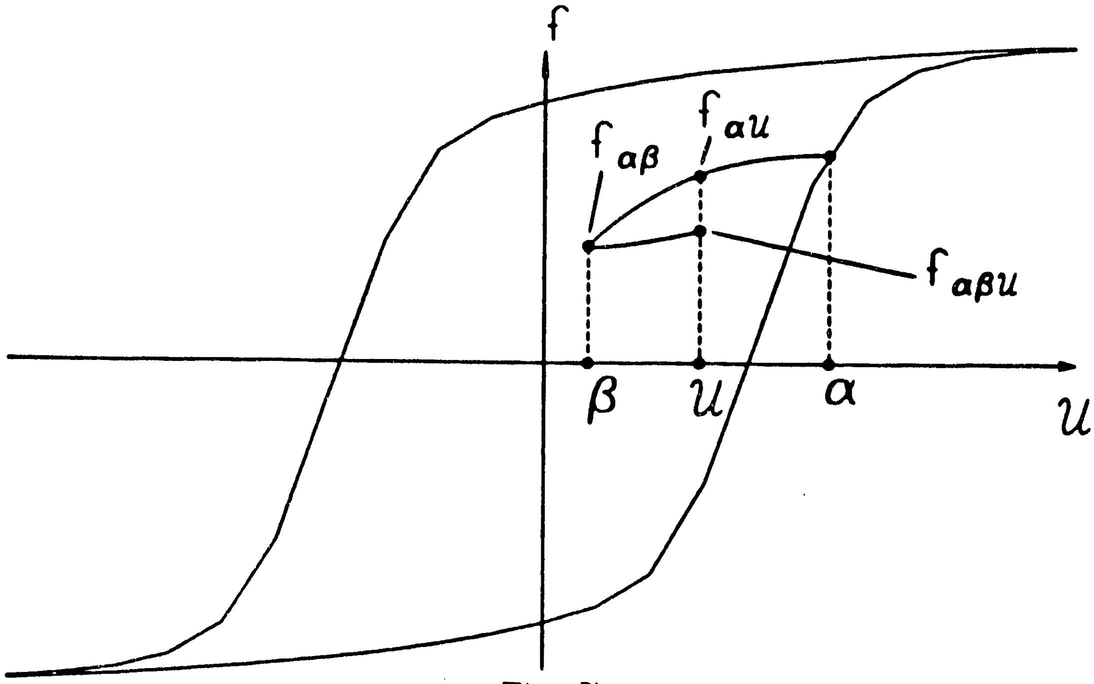
f
$f_{\alpha u}$
$f_{\alpha\beta}$
$f_{\alpha\beta u}$
β
u
α
u
Fig. 7

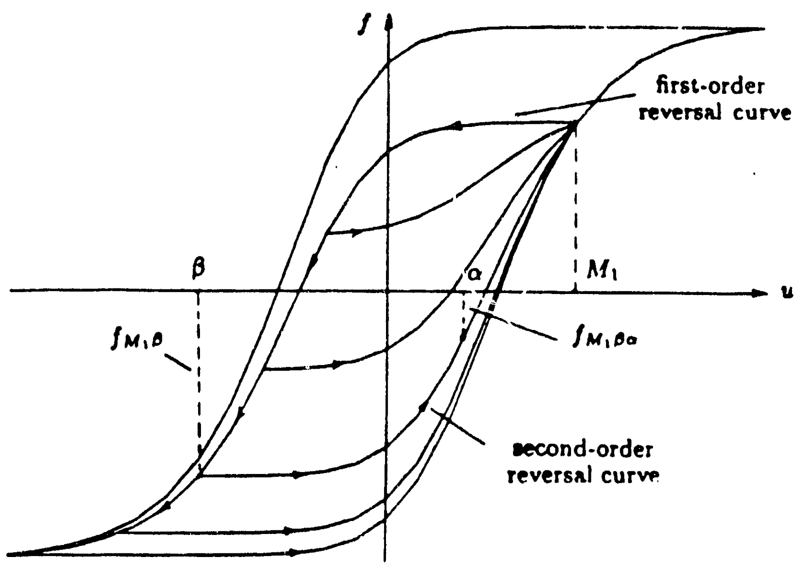
f
first-order
reversal curve
β
α
M_1
u
$f_{M_1\beta}$
$f_{M_1\beta\alpha}$
second-order
reversal curve
Fig. 8

All minor loops resulting from back-to-forth input variations between the same two consecutive extrema have equal vertical chords (output increments) for the same input values (Fig. 6).

It turns out that the Properties A and C are characteristic for the nonlinear Preisach model (7). This is revealed by the following result.

Representation Theorem

The wiping-out property and the property of equal vertical chords for minor loops constitute the necessary and sufficient conditions for the representation of a hysteresis nonlinearity by the nonlinear Preisach model on the set of piecewise monotonic inputs.

The identification problem of finding the function $\mu(\alpha, \beta, u)$ in (7) can be solved by employing experimentally measured first- and second-order transition curves shown in Fig. 7. By using these curves the following function can be defined:

$$P(\alpha, \beta, u) = f_{\alpha u} - f_{\alpha \beta u}, \tag{8}$$

which has the meaning of output increments between the first- and second-order transition curves. It can be shown that the function $\mu(\alpha, \beta, u)$ can be retrieved from $P(\alpha, \beta, u)$ by means of the formula:

$$\mu(\alpha, \beta, u) = -\frac{1}{2} \frac{\partial^2 P(\alpha, \beta, u)}{\partial \alpha \partial \beta}. \tag{9}$$

As far as numerical implementation of the model (7) is concerned, it can be carried out by using directly the function $P(\alpha, \beta, u)$ and by avoiding its differentiation as well as numerical evaluation of double integrals in (7). The appropriate formula for this purpose is given below:

$$f(t) = f^{-}_{u(t)} + \sum_{k=1}^{n(t)} [P(M_{k+1}, m_k, u(t)) - P(M_k, m_k, u(t))]. \tag{10}$$

Here, M_k and m_k are stored local input maxima and minima, respectively.

On the basis of the above discussion, it can be concluded that the nonlinear Preisach model (7) has the following advantages over the classical model. First, the congruency property of minor loops is relaxed for the nonlinear model. This results in a broader area of applicability of this model as compared with the classical model. Secondly, the nonlinear model allows one to fit experimentally measured first- and second-order curves. Since higher-order reversal curves are "sandwiched" between first- and second-order reversal curves, it is natural to expect that the nonlinear model will be more accurate than the classical one. This has been confirmed by experimental testing of Preisach-type models (see [4], [5]).

Before we have discussed the nonlinear Preisach model of hysteresis which is a far-reaching generalization of the classical Preisach model. This generalization has been achieved by assuming that the distribution function μ is dependent of the current value of input $u(t)$. Another approach to the generalization of the classical Preisach model is to assume that the function μ depends on stored past extremum values of input, $\{M_k, m_k\}$. This approach has been recently and briefly explored in [6]. We have followed this approach as well, however, our treatment (see [5]) of the model itself and the identification problem for this has model deviates appreciably from the discussion in [6].

We shall largely restrict our discussion to the case when the function μ depends only on the first (largest) input maximum M_1. In this case, the Preisach-type model can be defined as follows:

$$f(t) = \iint_{T_{M_1}} \mu(\alpha, \beta, M_1)\hat{\gamma}_{\alpha\beta}u(t)d\alpha d\beta + \frac{f^+_{M_1} - f_-}{2}. \tag{11}$$

Here T_{M_1} is a triangle defined by inequalities $\beta_0 \leq \beta \leq \alpha \leq M_1$.

We shall use the following interpretation of the above model. For any fixed extremum M_1, the model (11) will be used to describe hysteresis behavior in the region confined between an ascending branch $f^+_{u(t)}$ and a first-order reversal curve $f_{M_1\beta}$ (see Fig. 8). For this reason, the model (11) can be termed as a "restricted" Preisach model of hysteresis. However, the above "restriction" does not diminish at all the region of applicability of the model. This is because M_1 may assume any value between β_0 an α_0.

Function $\mu(\alpha, \beta, M_1)$ can be found by matching second-order reversal curves $f_{M_1\beta\alpha}$ (see Figure 8). The appropriate formulas are the following:

$$F(\alpha, \beta, M_1) = \frac{1}{2}(f_{M_1\beta\alpha} - f_{M_1\beta}). \tag{12}$$

$$\mu(\alpha, \beta, M_1) = -\frac{\partial^2 F(\alpha, \beta, M_1)}{\partial\alpha\partial\beta}. \tag{13}$$

Numerical implementation of the model (11) can be carried out by using the formula:

$$f(t) = 2\sum_{k=1}^{n(t)}[F(M_k, m_{j-1}, M_1) - F(M_k, m_k, M_1)] + f_-, \tag{14}$$

that is without differentiation in (13) of experimentally obtained data and by avoiding evaluation of double integrals in (11).

It is clear that the model (11) has almost identical structure with the classical Preisach model. For this reason, it is apparent that the wiping-out property holds for the restricted model (11). However, the congruency property of minor hysteresis loops undergoes some modification. This modification can be described as follows. We call minor hysteresis loops comparable if they are formed as a result of back-and-forth input variations between the same consecutive reversal values and these input variations take place some time after the same largest input maximum was achieved. The given definition of comparable minor loops implies the possibility of different past input histories between the time when the largest maximum M_1 was achieved and the time when the above mentioned back-and-forth input variations commence. It can be proven that all comparable minor loops described by the restricted model (11) are congruent. It is clear from the above statement that the congruency of minor hysteresis loops prescribed by the model (11) is to a certain extent history dependent. This is not the case for the classical Preisach model.

It turns out that the wiping-out property and the modified congruency property are characteristic for the restricted model (11) in a sense that the following result is valid.

Representation Theorem

The wiping-out property and the congruency property of comparable minor loops constitute necessary and sufficient conditions for the representation of actual hysteresis nonlinearities by the restricted Preisach mode (11).

It is clear that the modified congruency property is more general than the congruency property of the classical Preisach model. Thus the restricted model (11) is more general than the classical one. In addition, the restricted model (11) allows one to fit experimentally measured first- and second-order reversal curves, while the classical Preisach model is able to fit only first-order reversal curves. Since higher-order reversal curves are "sandwiched" between first- and second-order reversal curves, it is natural to expect that the restricted model will be more accurate than the classical Preisach model.

It is clear from the previous discussion that higher-order restricted Preisach models of hysteresis can be defined as:

$$f(t) = \iint\limits_{T_{M_1 m_1 \ldots M_k}} \mu(\alpha, \beta, M_1, m_1, \ldots M_k) \hat{\gamma}_{\alpha\beta} u(t) d\alpha d\beta + C_{M_1 m_1 \ldots M_k}. \tag{15}$$

It is apparent that higher-order transition curves can be used for the determination of the function $\mu(\alpha, \beta, M_1, m_1, \ldots M_k)$ and $C_{M_1 m_1 \ldots M_k}$. It goes without saying that by increasing the order of the restricted Preisach model we can increase the accuracy of this model. However, this increase in accuracy is amply paid for by the increase in the amount of experimental data which is required for the identification of higher-order models. For this reasons, the use of restricted Preisach models of order higher than two does not seem to be practically feasible or attractive.

So far our discussion has been centered around the classical and generalized Preisach models of hysteresis which are static in nature. The term "static" implies that in these models only past input extrema leave their mark upon the future values of output, while the speed of input and output variations has no influence on branching. Some research has been performed to relax the "static property" of Preisach-type models. As a result new Preisach-type models which are applicable to the description of dynamic hysteresis have been developed (see [7]). For instance, the "dynamic" generalization of the classical Preisach model is given by:

$$f(t) = \tilde{f}(t) + \frac{df}{dt} \iint\limits_{\alpha \geq \beta} \mu_1(\alpha, \beta) \hat{\gamma}_{\alpha\beta} u(t) d\alpha d\beta, \tag{16}$$

where the $\tilde{f}$-term stands for the static component of hysteresis nonlinearity:

$$\tilde{f}(t) = \iint\limits_{\alpha \geq \beta} \mu_0(\alpha, \beta) \hat{\gamma}_{\alpha\beta} u(t) d\alpha d\beta. \tag{17}$$

The expressions (16) and (17) are transparent from the physical point of view. They show that the instant speeds of output variations are directly proportional to the differences between instant and static output values.

We next discuss the identification problems of determining the μ_0- and μ_1-functions by fitting the models (16) and (17) to some experimental data. The following experiments are used to solve this problem. Starting from the state of negative saturation, the input $u(t)$ is monotonically increased until it reaches some value α at $t = t_0$ and it is kept constant for $t \geq t_0$. As the input is being kept constant, the output relaxes from its value f_α at $t = t_0$ to its static value $\tilde{f}_\alpha$. According to the model (16), this relaxation process is described by the differential equation:

$$\tau_\alpha \frac{df}{dt} + f = \tilde{f}_\alpha, \tag{18}$$

where τ_α has the meaning of relaxation time and can be experimentally measured.

Next, the hysteresis nonlinearity is brought back to the state of negative saturation. Starting from this state, the input is again monotonically increased until it reaches the value α. Then the input is monotonically decreased until it reaches some value β at time $t = t_0'$ and it is kept constant for $t > t_0'$. As the input is being kept constant, the output relaxes from its value $f_{\alpha\beta}$ at $t = t_0'$ to its static value $\tilde{f}_{\alpha\beta}$. The model (16) yields the following differential equation for the above relaxation process:

$$\tau_{\alpha\beta} \frac{df}{dt} + f = \tilde{f}_{\alpha\beta}, \tag{19}$$

where $\tau_{\alpha\beta}$ has also the meaning of relaxation time and can be experimentally measured.

We introduce the function

$$q(\alpha, \beta) = \tau_\alpha - \tau_{\alpha\beta}. \tag{20}$$

Then, it can be shown that:

$$\mu_1(\alpha, \beta) = -\frac{1}{2} \frac{\partial^2 q(\alpha, \beta)}{\partial\alpha\partial\beta}. \tag{21}$$

As far as the determination of the μ_0-function in (17) is concerned, it can be performed in exactly the same way as for the classical Preisach model (1), that is by using first-order reversal curves (see (3) and (4)). This is so because for very slow (quasi-static) input variations the dynamic model (16)-(17) is reduced to the classical model (1).

Dynamic generalizations of nonlinear and restricted Preisach models as well as the solution of identification problems for them can be accomplished in a similar fashion as for the model (16)-(17).

The Preisach-type models previously described exhibit the wiping-out property. This property results in an immediate formation of minor hysteresis loops after only one cycle of back-and-forth input variations between any two consecutive extremum values. However, experiments show that hysteresis loop formations are often preceded by some stabilization process which may require appreciable number of cycles before a stable minor loop is achieved. This stabilization process is often called in the literature "accommodation" or "reptation" process. Sometimes this accommodation process can be appreciable and then it is important to model it. A certain modification of the moving Preisach model has been developed which allows one to account for the accommodation process.

The Preisach model with accommodation is defined as:

$$f(t) = \iint\limits_{R_{u(t)}} \mu(\alpha, \beta, f^{(m)})\hat{\gamma}_{\alpha\beta}u(t)d\alpha d\beta + r(u(t)). \tag{22}$$

In the previous formula $r(u(t))$ stands for a fully reversible component which is represented by some single-valued function of $u(t)$, while:

$$f^{(m)} = M_k^f \quad \text{if} \quad (\alpha, \beta)\epsilon R_k(t), \tag{23}$$

where M_k^f are local extremum values of output f and $R_k(t)$ are rectangular regions formed after the extremum M_k^f had been achieved (see Figure 9). It is easy to see that the regions $R_k(t)$ are reduced with time and can even be completely wiped out. This fact is reflected in (23) by indicating that R_k are dependent of t. It is also clear from Figure 9 that M_k^f are local output minima for even k and local maxima for odd k.

It can be easily proved that the model (22) does account for the accommodation process (see Figure 10).

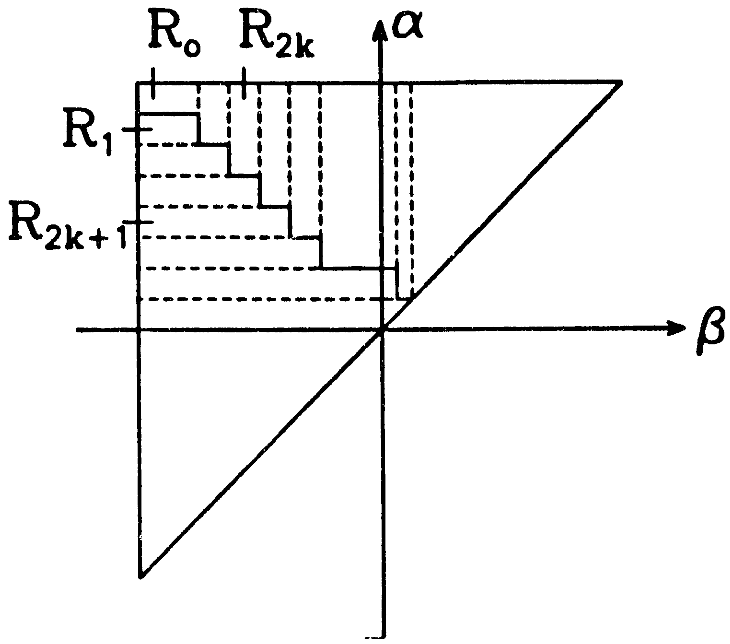

Fig. 9

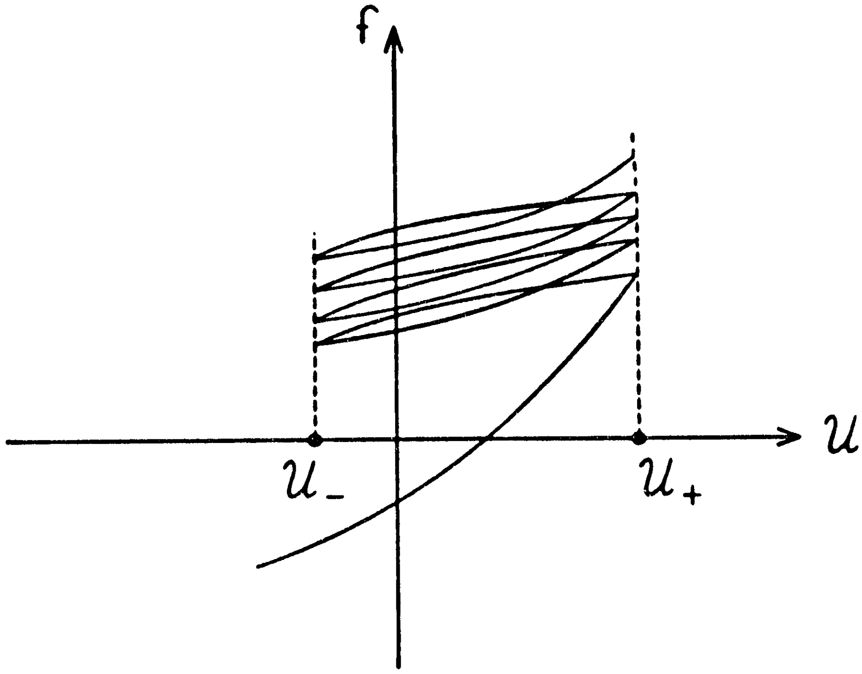

Fig. 10

We next proceed to the discussion of the identification problem. It turns out that the model (22) - (23) is very general in nature and it is not clear at this point how to solve the identification problem for this model. However, the identification problem becomes tractable if the dependence of μ-function on $f^{(m)}$ is factored out. In this way, we arrive at the following model:

$$f(t) = \iint\limits_{R_{u(t)}} \nu(f^{(m)})\mu(\alpha,\beta)\hat{\gamma}_{\alpha\beta}u(t)d\alpha d\beta + r(u(t)), \tag{24}$$

where: $f^{(m)}$ are defined in the same way as in (23), and ν-function is assumed to be known. Thus the identification problem consists in determining the functions $r(u)$ and $\mu(\alpha,\beta)$ by fitting the model (24) to some experimental data. It can be shown that these functions can be found by using the following expressions:

$$r(u) = \frac{\nu(f_+)f_u^+ + \nu(f_-)f_u^-}{\nu(f_+) + \nu(f_-)}, \tag{25}$$

$$\mu(\alpha,\beta) = -\frac{\partial^2 T(\alpha,\beta)}{\partial\alpha\partial\beta}, \tag{26}$$

where:

$$T(\alpha,\beta) = \frac{\nu(f_\alpha)[f_\beta^- - r(\beta)] - \nu(f_+)[f_{\alpha\beta} - r(\beta)]}{\nu(f_+)[\nu(f_\alpha) + \nu(f_-)]}, \tag{27}$$

while f_+ and f_- are the output values in the states of positive any negative saturation, respectively, f_β^- represents the limiting descending branch and $f_{\alpha\beta}$ stands (as before) for first-order reversal curves.

Our ongoing research has also been focused on the mathematical modeling of vector hysteresis. The main research in the area of vector hysteresis modeling has long been centered around the classical Stoner-Wohlfarth (S-W) model. As a result, this model has further been developed and used in the area of magnetic recording. It is known that the S-W model is constructed as an ensemble of particles with symmetrical loops. For this reason, this model does not describe nonsymmetrical minor loops. This difficulty is often attributed to the fact that the S-W model does not account for "particle interactions."

Furthermore, the S-W model does not address the question what part of the past history leaves its mark upon the future. The above question is very important for the understanding of the phenomenological nature of vector hysteresis. Furthermore, the identification problem of finding the distribution function by fitting the S-W model to some experimental data has not been adequately addressed yet. Solutions to this problem are usually achieved by some artwork rather than by using a well-established procedure.

Our research was motivated by the desire to circumvent the difficulties mentioned above. As a result, new vector Preisach models of hysteresis have been developed. These models are based on the notion that past extremum values of input projections along all possible directions may leave their mark upon the future values of output. To detect and accumulate the past extremum values of input projections, the scalar Preisach models (Preisach's particles) are used. These models are continuously distributed along all possible directions. Thus, the scalar Preisach model is the main building block for the vector model, which is constructed as a superposition of scalar models. Since the scalar Preisach model describes nonsymmetrical minor loops, the same property is inherited by the vector Preisach model. In this manner, the vector Preisach model takes the "particle interactions" into account on the phenomenological level. Moreover, if the input is restricted to vary along only one direction, then it can be shown that the vector model exhibits the properties of the scalar model. In this sense, the vector model is reduced to the scalar model. This reduction is valuable because the scalar Preisach model has long been considered as a fairly good model for scalar hysteresis.

Using the idea described above, the 3-D and 2-D vector Preisach model can be represented respectively, as follows:

$$\vec{f}(t) = \int_0^{2\pi} \int_0^{\pi/2} \vec{e}_{\theta,\varphi} \left(\iint_{\alpha \geq \beta} \nu(\alpha, \beta, \theta, \varphi) \hat{\gamma}_{\alpha\beta} u_{\theta,\varphi}(t) d\alpha d\beta \right) \sin\theta d\theta d\varphi, \tag{28}$$

$$\vec{f}(t) = \int_{-\pi/2}^{\pi/2} \vec{e}_{\varphi} \left(\iint_{\alpha \geq \beta} \nu(\alpha, \beta, \varphi) \hat{\gamma}_{\alpha\beta} u_{\varphi}(t) d\alpha d\beta \right) d\varphi, \tag{29}$$

where $\vec{e}_{\theta,\varphi}$ is a unit vector along the direction specified by spherical coordinates θ and φ,

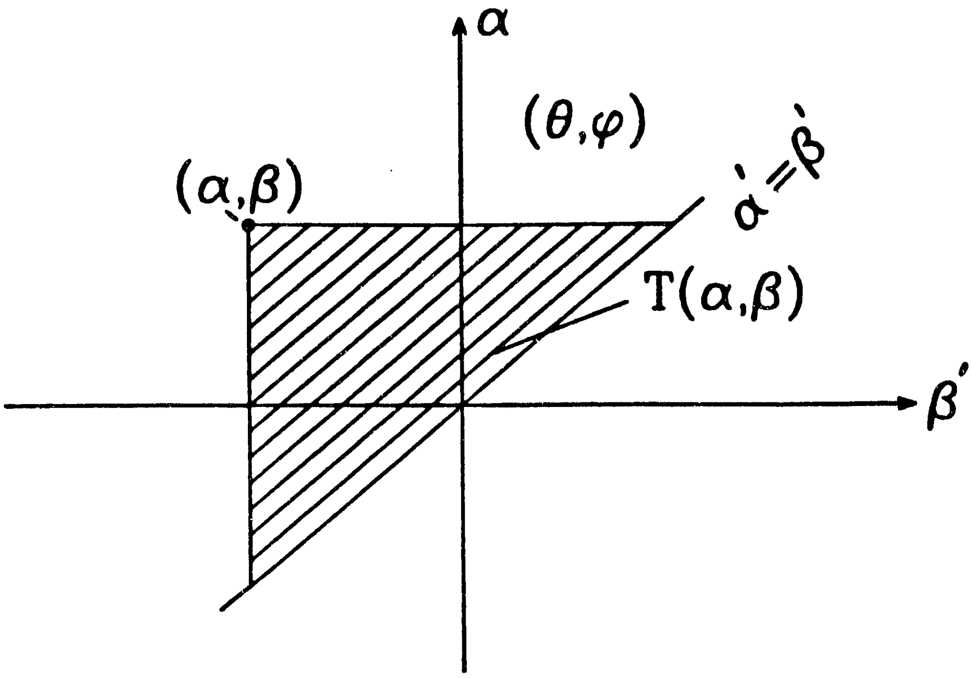

α'
(θ,φ)
(α,β)
$\alpha'=\beta'$
$T(\alpha,\beta)$
β'

Fig. 11

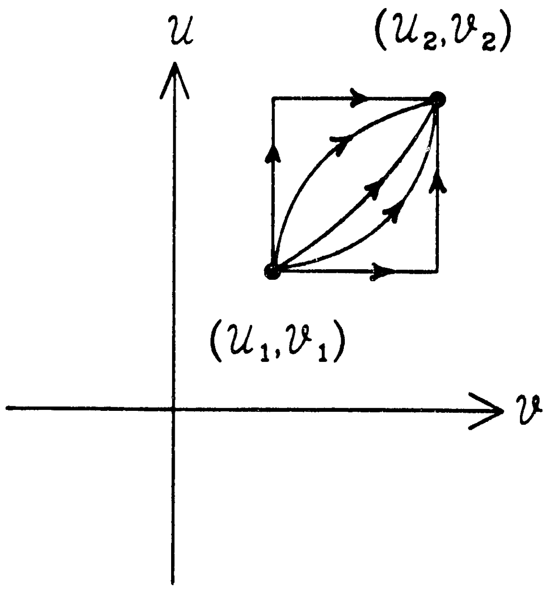

u
(u_2,v_2)
(u_1,v_1)
v

Fig. 12

and $u_{\theta,\varphi}(t)$ is the projection of vector input $\vec{u}(t)$ along the direction of $\vec{e}_{\theta,\varphi}$; $\vec{e}_\varphi$ and $u_\varphi(t)$ have similar meanings for the 2-D model (29).

In the models described above, the functions ν have not yet been specified. These functions should be determined by fitting the vector models to some experimental data. This is an identification problem. It is apparent that the identification problem is the central one as far as practical applications of the above vector hysteresis models are concerned. The solution of the identification problem is significantly simplified by the introduction of the auxiliary function $P(\alpha, \beta, \theta, \varphi)$. For any fixed θ and φ, consider a triangle $T(\alpha, \beta)$ shown in Figure 11. Then by definition:

$$P(\alpha, \beta, \theta, \varphi) = \iint_{T(\alpha,\beta)} \nu(\alpha', \beta', \theta, \varphi) d\alpha' d\beta'. \tag{30}$$

By using (30), it can easily be shown that P is related to ν by the formula:

$$\nu(\alpha, \beta, \theta, \varphi) = -\frac{\partial^2 P(\alpha, \beta, \theta, \varphi)}{\partial\alpha\partial\beta}. \tag{31}$$

Thus, if the function P is somehow determined, then the function ν can be easily retrieved. However, from the computational point of view, it is more convenient to use the function P than ν. This is because the double integrals with respect α and β in expressions (28) and (29) can be explicitly expressed in terms of P, and in this way the above double integration can be completely avoided.

It turns out that the identification problem can be reduced to the solution of special integral equations which relate the function $P(\alpha, \beta, \theta, \varphi)$ to some "unidirectional" (scalar) hysteretic data. In the case of **isotropic** models, these data are provided by the set of first-order reversal curves (see Fig. 3) measured along arbitrary direction. By using these curves and introducing the function

$$F(\alpha, \beta) = \frac{1}{2}(f_\alpha - f_{\alpha\beta}), \tag{32}$$

the following integral equations have been derived for 3-D and 2-D models, respectively:

$$\int_0^{\pi/2} \cos\theta \sin\theta P(\alpha\cos\theta, \beta\cos\theta) d\theta = \frac{1}{2\pi} F(\alpha, \beta), \tag{33}$$

$$\int_{-\pi/2}^{\pi/2} \cos\varphi P(\alpha\cos\varphi, \beta\cos\varphi)d\varphi = F(\alpha, \beta). \quad (34)$$

These integral equations have a peculiar structure which has been exploited in order to find their analytical sol .tions. These solutions for 3-D and 2-D models, respectively, are given below:

$$P(\alpha, \lambda\alpha) = \frac{1}{2\pi\alpha}\frac{d}{d\alpha}[\alpha^2 F(\alpha, \lambda\alpha)], \quad (35)$$

$$P(\alpha, \lambda\alpha) = \frac{1}{\pi\alpha}\frac{d}{d\alpha}\int_0^\alpha \frac{s^2 F(s, \lambda s)}{\sqrt{\alpha^2 - s^2}}ds, \quad (36)$$

where $\lambda = \beta/\alpha$.

The identification problem for **anisotropic** Preisach model has turned out to be more challenging. This is especially true for 3-D anisotropic models where some facts from the theory of irreducible representations of the group of rotations of 3-D Euclidian space have proved to be very instrumental.

The main idea for the solution of the identification problem has been to relate the function $P(\alpha, \beta, \theta, \varphi)$ to the first-order transition curves experimentally measured along all possible directions $\vec{e}_{\theta,\varphi}$. These curves can be characterized by the function:

$$F(\alpha, \beta, \theta, \varphi) = \frac{1}{2}(f_{\alpha\theta\varphi} - f_{\alpha\beta\theta\varphi}). \quad (37)$$

It has proved to be convenient to use spherical harmonic expansions for the functions P and F:

$$P(\alpha, \beta, \theta, \varphi) = \sum_{k=0}^{\infty}\sum_{m=-k}^{k} P_{km}(\alpha, \beta)Y_{km}(\theta, \varphi), \quad (38)$$

$$F(\alpha, \beta, \theta, \varphi) = \sum_{k=0}^{\infty}\sum_{m=-k}^{k} F_{km}(\alpha, \beta)Y_{km}(\theta, \varphi), \quad (39)$$

where $Y_{km}(\theta, \varphi)$ are spherical harmonics, while P_{km} and F_{km} are corresponding expansion coefficients.

By using the above expansions and some facts from the theory of irreducible representations of the group of rotations, the following integral equations which relate P_{km} to F_{km} have been derived:

$$\int_0^{\pi/2} P_{km}(\alpha\cos\xi, \beta\cos\xi) L_k(\cos\xi)\cos\xi\sin\xi d\xi = \frac{(-1)^m}{2\pi} F_{m}, (\alpha, \beta), \tag{40}$$

where L_k are Legendre polynomials.

Explicit analytical solutions to the equations (40) have be found for the cases $k = 0$ and $k = 1$. These solutions are given by:

$$P_{00}(\alpha, \lambda\alpha) = \frac{1}{2\pi\alpha}\frac{d}{d\alpha}[\alpha^2 F_{00}(\alpha, \lambda\alpha)], \tag{41}$$

$$P_{1m}(\alpha, \lambda\alpha) = \frac{(-1)^m}{2\pi\alpha^2}\frac{d}{d\alpha}[\alpha^3 F_{1m}(\alpha, \lambda\alpha)], \qquad (m = \pm 1, 0), \tag{42}$$

where again $\lambda = \beta/\alpha$.

Thus, if we are interested only in the first four terms of spherical harmonic expansion for P (this is a first-order approximation for anisotropic media), then the explicit analytical solution for the identification problem is given by formulas (41) and (42).

For $k > 1$, equations (40) can be solved numerically. Discretization procedures can be applied directly to equations (40), or these equations can first be reduced to the Volterra equation of the second kind:

$$P_{km}(\alpha, \lambda\alpha) - \int_0^{\alpha} P_{km}(x, \lambda x)\frac{x}{\alpha^3} L'_k\left(\frac{x}{\alpha}\right) dx =$$
$$= \frac{(-1)^m}{2\pi\alpha}\frac{d}{d\alpha}\left[\alpha^2 F_{km}(\alpha, \lambda\alpha)\right]. \tag{43}$$

The vector Preisach models discussed above have been constructed as superpositions of classical scalar Preisach models continuously distributed along all possible directions. For this reason, the above vector Preisach models have inherited some deficiencies of the classical scalar Preisach model. To eliminate these deficiencies, more sophisticated vector Preisach models have been designed. In these vector models nonlinear and restricted scalar

Preisach models, continuously distributed along all possible directions have been used. A thorough mathematical study of these vector Preisach models have been undertaken and the results similar to those discussed above have been obtained. Detailed discussion of the vector Preisach models can be found in publications [8], [9], [10] as well as in our book [11] "Mathematical Models of Hysteresis" recently published by Springer-Verlag.

The given review does not cover all the obtained results but rather is representative of what has been achieved in the course of our ongoing research. This review does not cover, for instance, such topics as Preisach models and superconducting hysteresis, Preisach modeling of magnetostrictive hysteresis, Preisach approach to the modeling of viscosity in hysteretic systems, experimental testing of Preisach models and software development, calculation of magnetostatic fields in media with hysteresis, etc. All these topics have been more or less extensively studied in the course of our work. Some of the results obtained in these areas will be discussed in the next section of this proposal because of their direct relevance to our plans for future research.

DATE
FILMED
12/23/92